4. INSTRUMENTATION

4.1 Accelerator

4.1.1 The TRITRON Development

M. Arnold, N. Baßmann, L. Beck, A. Cazan, A. Ferchau, G. Hinderer, P. Hofmann, E. Jakubowska, F. Klinkenberg-Haaß, L. Kopilarov, H.-J. Körner, B. Köppl, R. Kratz, J. Labedzki, B. Russ, P. Schütz, H. Seeger, U. Trinks, B. Walchshäusl

Summary

- The assemblage of the superconducting cyclotron Tritron is under way. In March 93 one third of the complete machine was mounted in the final position inside the vacuum vessel.
- The last three rf–cavities were electroplated with PbSn. The fourth cavity was conditioned successfully, the design values were reached. The remaining cavities will be conditioned at the final positions inside the vacuum vessel. All rf–couplers with driver systems and the controllable sapphire rods for the fine tuning were produced.
- All magnet sectors and the three injection channel magnets are ready for installation. Representative field measurements of radially defocusing channels of a complete sector gave results as good as those observed before from radially focusing channels [1]. The oscillating fields mentioned in Jahresbericht 91 were caused by a current dependent bypass at the upper end of the current leads, it is removed now.
- The beam guiding system from the tandem to the Tritron was taken into operation. The beam has the expected cross section values at the different profile monitors. The post–buncher was completed and then tested successfully, yet without beam.
- The Tritron vacuum vessel was prepared for the final assemblage of the machine. All flanges with feedthroughs for rf–power, magnet currents, potential wires, temperature sensors, driving rods etc. are installed. Almost all cables are laid inside of the vessel and outside to the local control desk.
- Six supporting steel platforms were manufactured. Below each platform two magnet sectors are suspended at prefixed horizontal positions. One cavity is inserted between the magnets and adjusted relatively to them, taking into account the different thermal contractions. The magnet sectors and the cavity can be adjusted axially within ± 0.1 mm relatively to the platform. In March 93 two complete units were put to the final positions below the ring shaped liquid helium reservoir inside the vacuum vessel. Before all pipes for the thermal siphon cooling had been attached, and steel covers were put on the magnet sectors to shield the cavities from stray fields of the current leads. A device was constructed, by which the axial position of all cavities and magnet sectors can be checked with a precision of ~ 0.1 mm inside the vacuum vessel even at low temperature.

- The beam position probes were tested successfully with ion beams (at $\simeq$ 300 K) and a laser beam (at $\simeq$ 10 K and $\simeq$ 300 K). With $^{16}O^{4+}$ of 25 MeV the position could be measured with a current as low as $\simeq 50 \cdot 10^{-12}$ A (particles). At a particle current of $\simeq 5 \cdot 10^{-9}$ A the resolution was $\pm$0.1 mm in radial and $\pm$0.2 mm in axial direction.

- Beam dynamic calculations have shown, that axial betatron resonance problems may occur at the innermost turns, where the axial betatron oscillation number crosses $Q_y = 1$. Vertical position errors of the magnets of $\sim$ 0.3 mm may lead to beam losses. As a precaution it is planned to supply the gradient windings of the magnets of one or both groups with current, thus shifting the betatron oscillation numbers. As a second more flexible tool small superconducting axial steerer magnets were designed. It is planned to install up to three steerer magnets per turn at least at the innermost turns. A prototype steerer magnet was produced. Field measurements at room temperature gave good results.

- A considerable amount of work was done on the development of the computer control system, especially for the rf–system, the current control of the magnets, and the control and reading of the position probes.

- Some preliminary studies were made for a system of two resp. three Tritron–rings to accelerate high current proton beams up to $\sim$ 800 MeV [2].

The RF system

As described in Jahresbericht 91 the superconducting surfaces of two cavities had been dammaged. In March 92, these cavities and the seventh, the spare cavity were electroplated with PbSn at the GSI.

The fourth Tritron cavity was tested and conditioned for several times. It showed the typical behavior of a Tritron cavity: some multipacting levels at low accelerating fields, appearing every time the cryostat had been opened, were easy to be removed; strong high level multipacting, finally removable only after extented rf– and He–processing during several test periods; then field limitation caused by field emission. The fourth cavity shows now the expected high unloaded quality factor at low and medium field levels (e.g. $Q_o = 1 \cdot 10^9$ at $U_{20} =$ 222 kV) which indicates a high quality of the superconducting PbSn layer. However its maximum accelerating voltage is still limited at 650 kV by strong field emission. The field emission limit can be shifted to higher field levels by further He–conditioning.

Another technique of conditioning a cavity exposed to air is to heat it up from room temperature to 80^o C in vacuum, to remove water from the surface. Therefore two heating wires, integrated into the copper cooling pipes of the cavity were installed and tested.

During the last year a lot of detailed work was done also on the other parts of the rf–system including the post–buncher and the phase probe:

- motor–driven devices: The work on the input and output couplers and the saphir rods for the frequency fine tuning of the cavities was finished. A mechanical device for the frequency tuning of the cavity as described in Jahresbericht 91 was build and assembled with the first Tritron segment. All 24 motor–drives, belonging to the cavities, were manufactured and installed on the vaccuum vessel. The mechanical frequency tuning of the post–buncher was tested. The motor control system was installed and tested for 18 devices. Some electronical parts will be enlarged to serve the in total 25 motor drives (including the motor–drive for the buncher tuning).

- rf–power amplifier and feeder line: A watercooled device consisting of six 50 Ω dummy loads and six circulators was built and installed. An interface for the computer–control of the amplifiers was designed, built and tested.

- phase and amplitude control system (as described in Jahresbericht 89): Final adjustments and calibration of the demodulator and modulator parts, including the modified devices for the post–buncher, with regard to the range of the input and output signals was done. To turn the phase of the whole cavity system a computer controlled modified modulator is used as a phase shifter in the reference frequency line.

- frequency generating: The computer control of the signal generator was installed and tested. The three frequency generator supplies different signal levels, depending on the harmonic numbers. Therefore a computer controlled variable gain amplifier device was build and calibrated.

- devices for the linkage of the cavity system to the beam guiding system: To ensure constant signal levels the variable gain amplifier for the phase pickup signal was supplemented by a variable attenuator, both devices are computer controlled.
  A signal processing system was developed to correct energy deviations before the post–buncher by means of the phase deviations, measured by the pick–up probe.[3]

All computer controlled rf–system components are served from the same VME–bus computer. The first versions of the control codes were written for testing the single devices. The second version, with special regard to the management of the rf–system, error handling and communication with the Tritron control system is in stage of development.

The post–buncher

In the beam line between the MP–tandem pre–accelerator and the Tritron a post–buncher will be installed, which shall compress the nanosecond wide pulses emerging from the tandem to about 100 ps. The principal design and technical details about this buncher have been reported in Jahresbericht 88, 89 and [4, 5]. Here the main features of this buncher will be reviewed.

The buncher is a quarter wave resonator, operated at frequencies between 75 and 86 MHz. The frequency variation is due to a change of the effective length of the inner conductor. This is accomplished without sliding contacts by a capacitively coupled metallic tube inside the inner conductor. This tuning tube can be moved galvanically insulated under full rf–power. Therefore no extra fine tuning is necessary. The axis of the resonator is vertical. The beam passes horizontally through two drift tubes, which are radially attached to the outer conductor. The two acceleration gaps formed by the drift tubes and the inner conductor have different widths (20 and 60 mm). Due to different transittime factors this provides bunching even for low beam velocities, where the rf–phase changes by 2π during the transition between the gaps. The insulated tuning tube is slit for the beam passage.

During the last year the buncher has been completed and successfully tested [6]. The stainless steel vacuum vessel forming the outer conductor (diameter 0.9 m, height 1.5 m) was electroplated with copper at the GSI. The inner parts (water cooled inner conductor, air cooled tuning tube, drift tubes) were fabricated in the workshop of the accelerator laboratory. The coaxial copper tubes of the inner conductor had to be soldered (by a private company) in a vacuum oven to avoid to thermal stresses.

The 4 kW rf–amplifier for driving the buncher, which was delivered at the beginning of the year, had to be repaired several times. Finally the company decided to rebuild the whole amplifier. In December this new fully transistorized amplifier was delivered. The following tests on an ohmic load and on the buncher have been successfully so far. Minor changes in the design of the power combiner stage will be done.

Several measurements with low power have been performed on the buncher, e.g. field distribution in the accelerating gaps and the quality factor. The Q–values are 21000 at 85 MHz (where the tuning tube is hidden inside the inner conductor) and 19000 at 75 MHz – somewhat higher than expected. These values indicate that less than 2 kW rf–power will be necessary to reach the designed gap voltage of 90 kV. This corresponds to a maximum bunching voltage of 160 kV – due to the two gaps. In power tests with the new amplifier up to 3 kW rf–power has been fed into the buncher so far at 75 and at 85 MHz – limited by field emission. Several levels of multipacting could be overcome rather easily.

Resonance problems of the vertical motion

The ion beam will be traced through the 238 magnets along the spiral orbit by individual setting of the magnet currents with the help of the superconducting switches. The information needed for this procedure is delivered by the radial beam position probes, which are installed behind each second magnet. Therefore, in radial direction the beam can always be approximately centered in the channel magnets [7].

For the vertical motion correction elements had been foreseen originally only at the junction between the Tritron and the injection and extraction beam line. Further calculations including vertical position errors of the magnet sectors have shown the necessity of vertical steering elements inside the Tritron.

The vertical betatron oscillation numbers in the Tritron vary about linearily with the radius between $Q_y = 0.9$ at injection and $Q_y = 1.8$ at extraction (no current in the gradient windings). Vertical position errors of the magnets lead to horizontal field components B_x in the plane $y = 0$. As a result coherent vertical oscillations of the beam are generated. These oscillations will be enhanced at the crossing of the resonance $Q_y = 1$, if the distribution of the B_x – fields along the circumference contains a first harmonic component. For a fixed limit of the position errors the amplitude of such a first harmonic field component is largest, if the position errors are distributed according to a curve, which contains five sine waves along one circumference. This is due to the alternating gradients of the magnets. If, for example, the magnet sectors are vertically displaced in such a fifth harmonic order with an amplitude of 0.3 mm, a coherent beam oscillation with more than 15 mm amplitude is built up within the first 7–8 turns. As the vertical aperture in the magnets is only ±5.5 mm, this would lead to a total beam loss.

The coherent vertical deviations of the beam can be corrected by a series of small superconducting steering magnets. Calculations have been performed to simulate the optimization of the beam position with arrays of 20 steerers each, placed in the gaps between the segments of the Tritron. The vertical angle of the central ray of the beam is changed at the location of a steerer by that amount, which leads to a minimum in the squared sum of the deviations y at all probe positions up to the next steerer. The best result, of course, is obtained, if a steerer array is installed in each of the six segment gaps. However, already three arrays in series (in gap 4, 5 and 6, counted from the first cavity after injection) lead to quite satisfying results. For the example mentioned above, the 15 mm oscillation amplitude could be reduced to a deviation of less than ±0.8 mm at all probe positions (±1 mm inside the sector magnets). A symmetrical distribution of the arrays (in gap 2, 4 and 6) leads to larger displacements in the outer region (turns 12 to 20). This is due to the crossing of $Q_y = 1.5$, where this steerer configuration with half a betatron oscillation between two steerers is ineffective. In all cases the angle corrections by the steerers needed to counteract a fifth harmonic vertical displacement of the magnet sectors with an amplitude of 0.3 mm were less than 5 mrad.

The calculations mentioned above have been performed with perfect sector magnets, with no quadratic and higher order field contributions. The influence of those error components in the field expansion had been studied earlier for the Tritron with midplane symmetry ($B_x = 0$ for the central ray) [7, 8]. To investigate the combined action of quadratic field contributions and vertical displacements of the magnet sectors the first order simulation program was extended by second order field contributions and the option of tracing many particles through the Tritron. The particles are still transformed by first order matrices. But at the ends and at the centre of the magnets the averaged action of quadratic field contributions is respected by a corresponding change in the radial and axial angles of the particles. Tracing many particles through the Tritron, the minimum and the maximum in each of the six particle coordinates is recorded along the spiral orbit.

As a result of these calculations, the phase space distortion due to a quadratic field component in the magnets is considerably larger, if a first harmonic B_x field is present at the crossing of the $Q_y = 1$ resonance. In the previous example (fifth harmonic vertical displacement with 0.3 mm amplitude), after correcting with the steerers (gap 4, 5 and 6) a second order term was switched on at the ends of the magnets. The quadratic sextupole contribution to the field at $x = \pm 4$ mm was $4 \cdot 10^{-3}$ at incetion and $2 \cdot 10^{-3}$ at extraction[1]. Now 4000 particles were started with coordinates on the surface of the phase space (eigenellipsoid with emittances of 3 π mm mrad in x, y, and z). About one third of the particles of this outer shell of the phase space were stopped, most of them in the vertically focusing magnets on the innermost turns. With the same quadratic term but no vertical displacement of the magnets all particles were passed through the Tritron, with only slightly enlarged envelopes compared to the linear calculation. This is in agreement with the previous investigations [8]. Measurements of the quadratic sextupole contributions gave $\leq 10^{-3}$ for both types of channel magnets [1]

A series of further calculations has been performed with changes in the oscillation numbers in order to shift Q_y beyond the $Q_y = 1$ resonance. This can be done by supplying the gradient windings with currents. The current in the gradient windings can be chosen for each type separately. The most suitable situation was found by increasing the absolute values of the gradients in all sector magnets with a gradient winding current of about 14 % of the average current in the main coils. This will change the normalized gradients $1/B \cdot \partial B/\partial r$ from $(3.6, -4.9)\mathrm{m}^{-1}$ to $(4.16, -5.66)\mathrm{m}^{-1}$ for the two types of sector magnets. The betatron oscillation numbers in that case vary between injection and extraction from 1.28 to 1.85 for Q_x and from 1.00 to 2.12 for Q_y. In the same calculation as above but with these new gradients none of the 4000 particles were lost. In this configuration however the $Q_y = 2$ resonance is crossed on the last two turns. To test this influence the calculation was repeated with a fourth harmonic vertical displacement of the magnet sectors (0.3 mm amplitude), which contributes a strong second harmonic B_x field. In that run less than 1 % of the particles were stopped on the last few turns.

A device to measure the vertical position of the sector magnets

The last chapter showed the importance of narrow tolerances in the vertical position of the magnet sectors to ensure the midplane symmetry of the system. For this purpose a measuring device was developed, which shall determine the vertical deviations of each sector to an accuracy of about 0.1 mm. It shall operate also when the Tritron is cooled down to liquid helium temperature. On each magnet sector three light emitting diodes with an aperture of 1 mm diameter will be mounted 160 mm below the medium plane – with an accuracy of about ±0.1 mm.

The vertical position of these diodes will be measured. A vertical cross section of the measuring device is shown in Fig. 1. It will be mounted on the central top flange of the Tritron vessel. An automatic levelling instrument (NI005A from Zeiss Jena) is positioned on a round plate, which can be rotated with respect to the vertical axis. The plate must be alligned only to ±3 mrad to ensure the optical axis of the instrument to be horizontal within ±1.5 μrad. By means of two pentagonal prisms the line of sight is transfered to a level at about 160 mm below the medium plane of the magnets – similar to the action of a periscope. The prisms are chosen as a pair with bending angles of about 90 degrees, however both identically within ±15 μrad.

[1] This is equivalent to a convexly curved field boundary with 18 mm radius at the entrance and exit of each magnet.

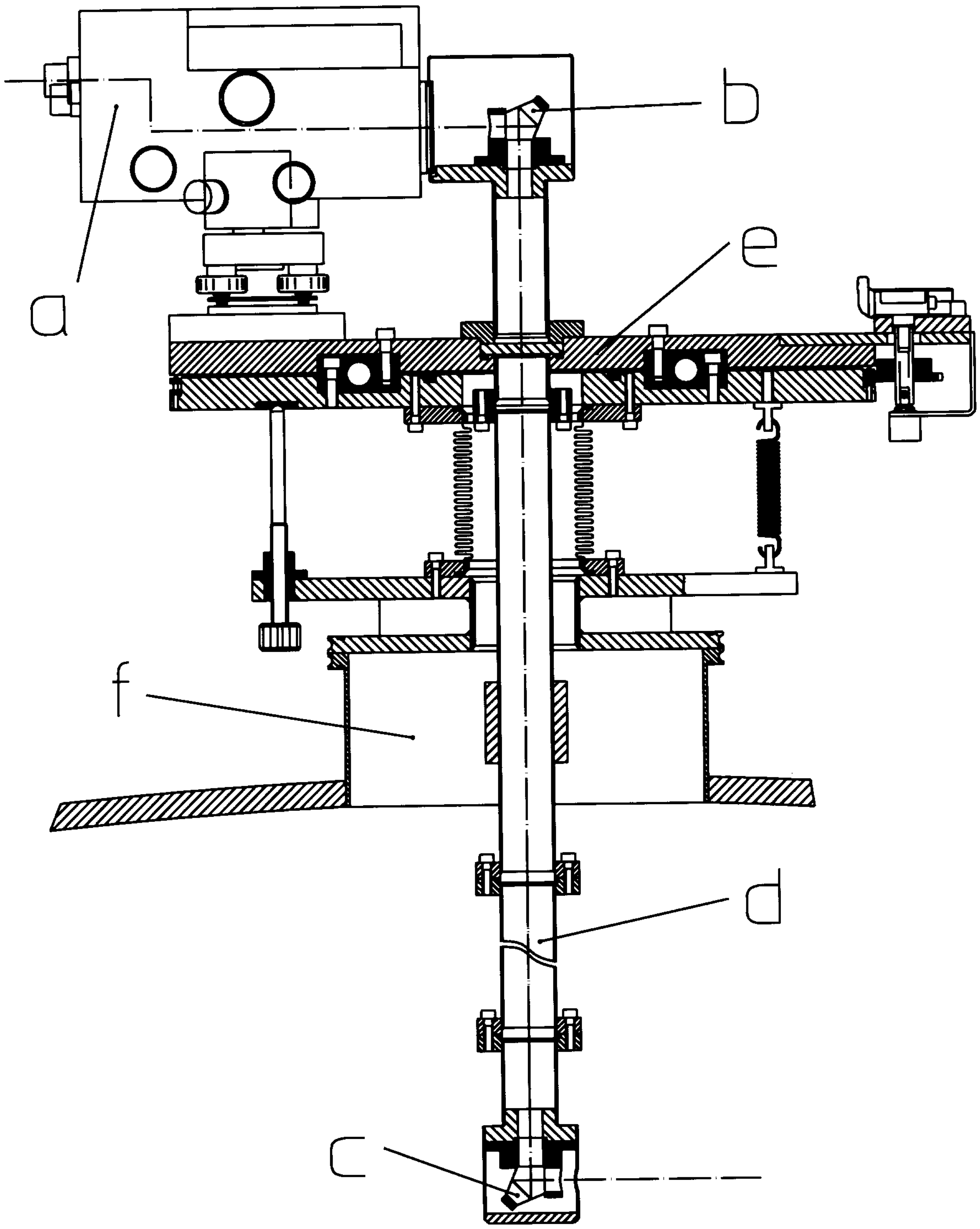

Fig. 1: The measuring device: a) automatic levelling instrument, b) upper pentagonal prism (warm), c) lower pentagonal prism (cold), d) demountable periscope tube, e) rotating plate (vacuum sealed), f) central top flange of the Tritron vessel.

Contrary to a deflection by two simple mirrors, these bending angles are independent from mounting tolerances and only determined by the angles between the glas surfaces of the prisms. Therefore e.g. a small bending of the tube, which holds the housing of the lower (cold) prism has no influence on the levelling. The knobs of the levelling instrument will be equipped with motor drives, and a small CCD camera replaces the ocular, which enables remote monitor control of the system. The vertical positions of the light emitting diodes below the medium plane are measured with the levelling instrument (measuring range ± 5 mm). Two extra diodes mounted with a hight difference of 160 mm allow measurements with respect to the reference level outside the Tritron. The lower diode can also be seen by the periscope, while the upper is observed from the outside through a window in the Tritron vessel near the medium plane.

The beam position probes

The first prototype of a unit with 20 probes, individually driven by one common bar, was often tested at low temperatures with a laser beam instead of a ion beam.

To improve the reliability some magnetic sensors (reed–contacts) were fixed at some crucial points and limit switches were placed at the endpoints of the bar. Further, the teflon–bearings have been substituted by those from carbon. Also the mechanical fixing of the support for the probes to the magnet sector was changed, so that the entire structure can be removed and placed easily.

The measurement precision in axial direction was increased by choosing another configuration of the tungsten–filaments.

The programs of the SUPER8–controlling processor were substantially changed and tested. Big parts were written in Z8–assembler, in order to speed them up. The SUPER8–processor controls the measurement and collects the data. To compute the beam position the full shape of the signals has to be analysed. As a result of many preliminary tests, and by carefully programming, the SUPER8–processor does this data processing fully automatic. Further, some extended error–checking routines were programmed in order to eliminate faulty measurements. The programs for the node–computer Z280 were written and tested. It manages up to 7 SUPER8–processors, resulting in a parallel structure of the beam probes controlling system.

Further more it connects the control desk computer via ARCNET with the SUPER8–processors and makes the final calculation of the beam position. For the control desk computer, the first program version was written and tested. It allows the user to start measurements, to read out the beam positions and to change all the important parameters such as: sampling rate, bar speed, amplitude etc. The measured signals can be displayed.

The entire system was built in such a manner, that it is self calibrating and that it delivers the beam position in millimeters.

Some electronic boards have been supplemented:
- the ADC–board was extended by an I/O–unit.
- the rf–calibration board was changed and tested.
- the switch–board for the coupling electromagnets of the probe bar was redesigned and tested.

The control system, as described above was used to test a single pendulum at room temperature with a 20 keV gold ion beam and with a 25 MeV oxygen ion beam. Both tests were successful. The lowest measured beam intensity was $50 \cdot 10^{-12}$ A (particles) and the measuring error was ± 0.1 mm in radial direction and better than ± 0.2 mm in axial direction.

[1] N.Baßmann, Diploma Thesis TUM, 1992
[2] U. Trinks, The superconducting separated–orbit cyclotron Tritron, 13^{th} Int. Conf. Cycl. and Appl., Vancouver, July 1992
[3] P. Pecher, Diploma Thesis TUM, 1992
[4] G. Hinderer and M. Leu, Nucl. Instr. and Meth. **A287** (1990) 287
[5] M. Leu, Diploma Thesis LMU, 1990
[6] P. Hofmann, Diploma Thesis TUM, 1993
[7] G. Hinderer, C. Rieß and U. Trinks, Nucl. Instr. and Meth. **A317** (1992) 13
[8] C. Rieß, Strahldynamik im Tritron, PhD Thesis TUM, 1990

4.1.2 Computer control for Tandem and Tritron

R. Assmann, L. Rohrer, H. Schnitter, B. Walchshäusl, J. Weigl

The computer control system for the tandem accelerator and the Tritron containing many small local computer crates communicating with the control desk computers ('386 and '486) via ARCnet as described earlier (Jahresbericht 1985 to 1991) has been developed further. Here the latest improvements will be presented.

Open Network FORTH ONF

The Open Network FORTH ONF has been improved by a faster dialog on the ARCnet. The time to parse an incoming message from ARCnet is decreased from approximately 6 ms to less than 1 ms. The conversion table, containing the symbolic addresses, is now stored in the non-volatile memory segment DS0 in the address-server. This has the advantage that a power failure on the address-server does not imply the necessity to download every node in the network to export their symbolic addresses. Also the conversion of the symbolic addresses into physical numbers is now faster.
Replacing the GEMforth by WINforth[2] is under discussion. WINforth, a Forth running under WINDOWS 3.1, has the following advantages:

1. A modern unique graphic user interface.
2. A cooperative multitasker.
3. Dynamic data exchange (DDE) between applications running under WINDOWS.
4. A lot of available application programs to analyze process data even on-line.
5. WINforth would run also on other hardware platforms under WINDOWS-NT.

[2] Laboratory Microsystems Inc.

File Server

One of the PCs in the network was dedicated as a file server. One can store and retrieve any file from and to all computers in the ARCnet. Special software was developed for two purposes: If all settings of the accelerator are correct, the data are stored so that they can be used later to set up the accelerator. The other application is the storage of mass spectra (beam current as a function of the field of the inflection magnet) of the beam coming from the injector. Comparison of the spectra taken at different times helps to evaluate how the ion source performance varies with time.

Beam Profile Monitors

The beam profile monitors (Danfysik Type 517) installed in the Tritron beam transport system were connected to the control system. The remote control of the BPM selector and the gain adjustment of the preamplifiers is done in the conventional way with relay boards in the control crate. A special ECB board, consisting of a fast ADC and a Zilog Super8-FORTH single board computer, was developed to digitize the scanned beam current. It stores the beam profile data temporarily so that they can be transmitted on request to the control desk. A data package representing a beam profile in horizontal and vertical plane contains 200 values, each 1 byte long. It can be routed in a single ARCnet page to the control desk within a few milliseconds. The control desk computer displays the beam profile graphically, the update rate being limited by the speed of the PC to 4 per second.

New Accelerator and Beam Transport Components

The new beam transport system between tandem and Tritron, and some of the existing accelerator subsystems (e.g. chopper and buncher at the low energy end of the tandem) were attached to the control system. For most purposes our standard I/O-boards in the local crates are used. The serial interface with data buffer developed last year is applied more and more often since many manufacturers equip their systems (magnet power supplies, magnetic field measuring instruments, vacuum gauges, vacuum pumps, etc.) with RS232 or RS485 interfaces.

A new I/O-board was developed in our laboratory to control the beam pulsing systems. This board replaces directly the microprocessor control unit which was used before, so that the remaining equipment can still be used without any modification.

An ARCnet board with a fiber optic link to the network has been developed and tested. It is planned to replace all coax ARCnet boards in the injector-tandem hall by ARCnet boards with a fiber optical link to prevent the damage of the electronic caused by a spark.

4.1.3 An optimized high current sputter ion source

A. Brunnhuber, G. Korschinek, A. Ulrich

An important parameter for the study of heavy–ion–beam–pumped laser mechanism is the energy deposited in the gas [1, 2]. For this purpose we have optimized the output of a high–current–type Cs–beam sputter–source [2]. Continuous and pulsed operation of the ion source have been compared, too. The main improvements were achieved by a reconstruction of the cylindrical tantalum–ionizer and a new extraction electrode as well. These yielded to less sparks at the extraction voltage of 30 kV. The corresponding optimized sputter voltage is 4 kV. The tests were performed with the high electro-negative elements sulphur and chlorine. Chlorine have been proved to yield the highest currents as expected and can be seen in table ??, too.

mode	continuous	pulsed
Ion		
$^{32}S^-$	80 μA	80 μA
$^{35}Cl^-$	150 μA	156 μA

Table 1: Values of measured ion currents

Furthermore investigations were performed on pulsed operation of the ion source [3]. The repetition rate was varied from 100 Hz up to 500 Hz, the variation of the pulse length was from 200 μs to 5 ms. The sputter voltage was studied in the range from 2 to 6 kV. Running the source in a pulsed mode didn't lead to remarkable enhanced ion currents. This is mainly due to an already well balanced ratio between the Cs condensation on the target and the ablation because of the Cs–sputter–beam in the continuous mode. An interesting effect was that the sputter-targets showed during pulsed–mode–operation a small hole ($\varnothing \approx 1$ mm) at the surface. The reason for that is the focussing of the Cs beam to the target surface by a space charged deformed electrical sputter-field. We can deduce that such a ion beam has a reduced emittance as well.

[1] A. Ulrich, J. Wieser, A. Brunnhuber, W. Krötz
Heavy ion beam pumped visible laser, Jahresbericht 1992
[2] A. Brunnhuber, Diplomarbeit, TUM, 1992
[3] A. Brunnhuber, G. Korschinek, A. Ulrich, Jahresbericht 1991, p. 134

4.1.4 Production of dense negative ion currents from laser produced plasma

T. Henkelmann and G. Korschinek

The possibility to produce dense negative ion currents from a laser produced plasma has been investigated for a wide area of target elements and different chemical compounds. To ensure equal conditions for all measurements, the laser ion source [1] was equipped with a revolving target wheel. Switching from one target material to another takes less than 3 seconds.

Whereas the mechanism of production of the negative ions seems to be the same, the extraction system and following ion optics has to be matched to each different target material. This can be traced back to the different amount of electrons released during a laser shot. The widely varying behavior of different target materials is due to a broad range of ionization energies and work functions of the elements and compounds used.

Though the maximum current achievable changes from target to target, all measurements show a common behavior related to the laser beam intensity (usually expressed in $\frac{W}{cm^2}$). The onset of negative ion production matches with the production of the first positively charged ions. This is a clear sign for plasma creation with a relative sharp threshold at $5 \cdot 10^7 \frac{W}{cm^2}$. With increasing laser intensity the negative ion current increases rapidly to the maximim current. However further enhancemant of the laser beam intensity decreases the ion yield and finally it vanishes completely.

As long as production occurs inside the plasma region, where high electron densities ($\sim 10^{19} cm^{-3}$) and corresponding high collision frequencies dominate all processes, the charge state distribution can be described by Saha equations:

$$\frac{n_e \cdot n_+}{n_0} = 2(\frac{m_e T_e}{2\pi\hbar})^{3/2} \cdot exp(-\frac{U_+}{T_e}) \qquad \frac{n_e \cdot n_0}{n_-} = 2(\frac{m_e T_e}{2\pi\hbar})^{3/2} \cdot exp(-\frac{U_-}{T_e})$$

where: n_0, n_+, n_- and n_e are the densities of neutral atoms, positive and negative ions and electrons;

U_+ and U_- are the energy of the first ionization level and the electron affinity;

T_e is the electron temperature measured in eV.

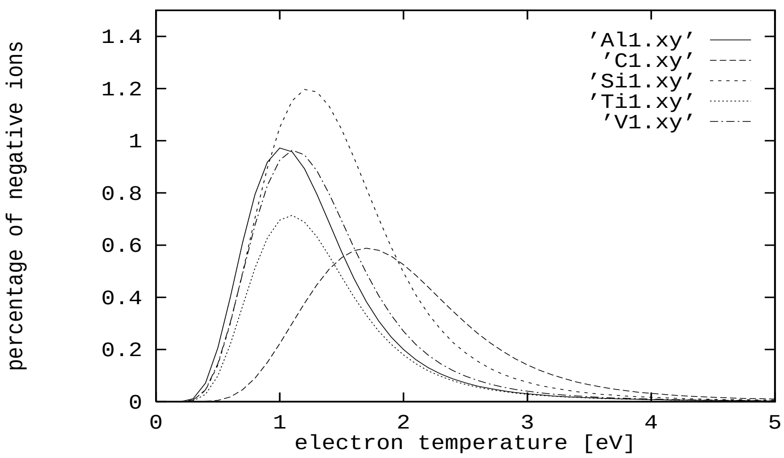

Fig. 1: Negative ion density vs. electron temperature for C, Al, Si, Ti and V.

In the following model the negative charge state is considered to be the zero point of ionization energy, i.e. the neutral atom is an 'ionized' state which ionization energy equals the electron affinity of the corresponding negative ion. Calculation of the Saha equilibrium distribution of charge states shows a behavior of negative ion formation in good agreement with the measurements. As observed there is a clear threshold with a rather steep slope for negative ion production and a decrease for further rising laser intensity, expressed in terms of the electron temperature (Fig. 1). The calculations shown here are valid for pure element targets. They look somewhat different for chemical compounds with two or more electron affinities and ionization levels.

Measurements have been done for a wide variety of elements. The usage of pure elements allows easy calculation of all partial energies necessary to build a negative ion as well as it suppresses the influence of chemical bindings and matrix effects. The maximum currents achieved so far with a time-of-flight distance of 0.5 m:

element	current in [μA]	element	current in [μA]
C	430	Ge	170
Mg	–	Nb	330
Al	170	Mo	90
Si	300	Pd	190
Cl	12000	Ag	200
V	320	In	420
Cr	150	Ta	180
Mn	–	Pt	180
Fe	350	Au	600
Ni	1700	Pb	620
Cu	1400	Bi	360

Mg- and Mn-targets have no measurable yield as expected because they do not form stable negative ions. The highest current was achieved for Cl^-. However this could not be done with a pure element but from NaCl as target material. Therefore a direct comparison with the other elements is not possible. Investigating one element in different chemical compounds is another approach to clarify the influence of ionization energy and thus of the amount of electrons available inside the plasma region. Current measurements are done with different salts of chlorine and iodine to optimize target material and extraction geometry of the laser ion source.

[1] T.Henkelmann and G.Korschinek, Jahresbericht 1990, 166